

Magnetic domain growth in a ferromagnetic Bose-Einstein condensate: Effects of current

Kazue Kudo¹ and Yuki Kawaguchi²

¹*Department of Information Sciences, Ochanomizu University,
2-1-1 Ohtsuka, Bunkyo-ku, Tokyo 112-8610, Japan*

²*Department of Applied Physics and Quantum-Phase Electronics Center,
University of Tokyo, 2-11-16 Yayoi, Bunkyo-ku, Tokyo 113-0032, Japan*

(Dated: May 25, 2022)

Magnetic domain patterns in a ferromagnetic Bose-Einstein condensate (BEC) show different properties depending on the quadratic Zeeman effect and dissipation. Another important factor that affects domain patterns and domain growth is superfluid flow of atoms. Domain growth in a ferromagnetic BEC with negative quadratic Zeeman energy is characterized by the same growth law as (classical) binary fluid in the inertial hydrodynamic regime. In the absence of the superfluid flow, the domain growth law for negative quadratic Zeeman energy is the same as that of scalar conserved fields such as binary alloys.

PACS numbers: 03.75.Kk, 03.75.Mn 03.75.Lm

I. INTRODUCTION

Domain growth laws due to domain coarsening has been studied in a wide variety of systems. Domain growths in ferromagnets, binary alloys, and binary fluids are typical examples. The equilibrium properties of a binary alloy as well as a ferromagnet with uniaxial anisotropy can be well modeled by the Ising model. However, the dynamics of domain coarsening in the binary alloy, where the population in each component is conserved, are different from that of non-conserved fields. For two-dimensional (2D) conserved scalar fields, the diffusive transport of the order parameter leads to the domain growth law $l(t) \sim t^{1/3}$, where l is the domain size and t is time, which is slower than the domain growth $l \sim t^{1/2}$ for non-conserved fields [1–4]. The situation is more complicated in a binary fluid where fluid flow also contributes to the transport of the order parameter. When diffusion dominates domain growth, the growth law reduces to that of binary alloy: $l \sim t^{1/3}$. However, $l(t) \sim t$ when the viscous force is dominant [5]. If the inertia of the fluid is important, the domain size grows as $l(t) \sim t^{2/3}$ [6].

Magnetic domain patterns are observed in a ferromagnetic Bose-Einstein condensate (BEC) as well as a ferromagnet. Recent techniques for imaging of magnetization profiles in ferromagnetic BECs have developed to investigate the real-time dynamics of magnetization, such as spin texture formation and nucleation of spin vortices [7–9]. A striking feature of a ferromagnetic BEC that is distinct from solid-state ferromagnets is that it supports superflow of constituent atoms. The purpose of this paper is to find out the effect of the superflow on the domain growth law. Spin dynamics of a ferromagnetic BEC is well described by Gross-Pitaevskii (GP) equation [10], which reduces to the hydrodynamic equation in the low energy limit. The hydrodynamic equation has been employed to investigate instabilities [11–13], config-

urations of skyrmions and spin textures [14, 15], and domain pattern dynamics [16]. In the presence of an energy dissipation, the hydrodynamic equation has essentially the same form as an extended Landau-Lifshitz-Gilbert (LLG) equation, which describes magnetization dynamics in conducting ferromagnets, where the electric current in the extended LLG equation corresponds to the superfluid current $n_{\text{tot}}\mathbf{v}_{\text{mass}}$ in the dissipative hydrodynamic equation [16–18]. The analogy between the dissipative hydrodynamic equation and the extended LLG equation has motivated us to investigate domain growth in ferromagnetic BECs.

In this paper, we investigate the effects of \mathbf{v}_{mass} on the magnetic domain growth in ferromagnetic BECs for Ising-like cases, where longitudinal magnetization is dominant. In our previous work, it was demonstrated that the superfluid flow has an effect to make domain formation faster when the longitudinal magnetization is dominant in a ferromagnetic BEC [16]. The focus of this work is on the scaling behavior of domain growth and the growth laws. We use both the hydrodynamic equation and the GP equation to investigate the magnetic domain pattern formation in (quasi-)2D systems. By making use of the hydrodynamic equation and artificially turning on and off the \mathbf{v}_{mass} term, we can find out the effect of \mathbf{v}_{mass} on the domain growth dynamics. We also discuss the effect of dissipation, which was originally introduced in a phenomenological manner.

The rest of the paper is organized as follows. We first introduce our model in Sec. II. In Sec. III, we briefly review the expected domain growth laws. Numerical simulations are given in Sec. IV. Our numerical simulations reproduce the expected domain growth laws. Conclusions are given in Sec. V.

II. MODEL

We consider a spin-1 BEC of N atoms under a uniform magnetic field applied in the z direction confined in a spin-independent optical trap $U_{\text{trap}}(\mathbf{r})$. The mean-field energy \mathcal{E} of the system is composed of the kinetic energy \mathcal{E}_{kin} , trapping potential energy $\mathcal{E}_{\text{trap}}$, the Zeeman energy \mathcal{E}_Z , and the interatomic interaction energy \mathcal{E}_{int} : $\mathcal{E} = \mathcal{E}_{\text{kin}} + \mathcal{E}_{\text{trap}} + \mathcal{E}_Z + \mathcal{E}_{\text{int}}$. The former three are respectively given by

$$\mathcal{E}_{\text{kin}} = \int d\mathbf{r} \sum_{m=-1}^1 \Psi_m^*(\mathbf{r}) \left(-\frac{\hbar^2}{2M} \nabla^2 \right) \Psi_m(\mathbf{r}), \quad (1)$$

$$\mathcal{E}_{\text{trap}} = \int d\mathbf{r} U_{\text{trap}}(\mathbf{r}) \sum_{m=-1}^1 |\Psi_m(\mathbf{r})|^2, \quad (2)$$

$$\mathcal{E}_Z = \int d\mathbf{r} \sum_{m=-1}^1 (pm + qm^2) |\Psi_m(\mathbf{r})|^2, \quad (3)$$

where $\Psi_m(\mathbf{r})$ is the condensate wave function for the atoms in the magnetic sublevel m , M is an atomic mass, and p and q are the linear and quadratic Zeeman energies per atom, respectively. The wave function is normalized to satisfy

$$\int d\mathbf{r} \sum_{m=-1}^1 |\Psi_m(\mathbf{r})|^2 = N. \quad (4)$$

Since the total longitudinal magnetization of an atomic cloud, which is isolated in vacuum, is conserved, the linear Zeeman effect merely induces the Larmor precession of atomic spins, which can be eliminated when we move onto the rotating frame of reference. Hence, we set $p = 0$ in this paper. On the other hand, the quadratic Zeeman energy is tunable by means of a linearly polarized microwave field and takes both positive and negative values [19, 20].

The interatomic interaction energy is given by

$$\mathcal{E}_{\text{int}} = \frac{1}{2} \int d\mathbf{r} [c_0 n_{\text{tot}}^2(\mathbf{r}) + c_1 |\mathbf{f}(\mathbf{r})|^2], \quad (5)$$

where

$$n_{\text{tot}}(\mathbf{r}) = \sum_{m=-1}^1 |\Psi_m(\mathbf{r})|^2, \quad (6)$$

$$f_\nu(\mathbf{r}) = \sum_{m,n=-1}^1 \Psi_m^*(\mathbf{r}) (F_\nu)_{mn} \Psi_n(\mathbf{r}) \quad (\nu = x, y, z), \quad (7)$$

are the number density and the spin density, respectively, with $F_{x,y,z}$ being the spin-1 matrices. The interaction coefficients c_0 and c_1 are related to the spin- S s -wave scattering length a_S as $c_0 = 4\pi\hbar^2(2a_2 + a_0)/(3M)$ and $c_1 = 4\pi\hbar^2(a_2 - a_0)/(3M)$. Here, we consider only the

short-range interaction and neglect the long-range magnetic dipole-dipole interaction (MDDI), since we are interested in the effect of the superfluid flow on the growth dynamics of magnetic domains, which is dominated by the interplay between the kinetic energy and the short-range (ferromagnetic) interaction. The MDDI is expected to determine the characteristic length scale of the magnetic structure in long-time dynamics, and therefore, unfavorable for the study of domain growth.

We first briefly review the magnetism of spin-1 BECs. The magnetism of spin-1 BECs is determined by the interplay between the spin-dependent interatomic interaction [the c_1 -term in Eq. (5)] and the quadratic Zeeman effect. It is obvious from Eq. (5) that, in the absence of the quadratic Zeeman effect, the condensate is fully-magnetized ($|\mathbf{f}| = n_{\text{tot}}$) for a negative c_1 , and non-magnetized ($|\mathbf{f}| = 0$) for a positive c_1 . The former is referred to as the ferromagnetic phase and the latter is the polar or antiferromagnetic phase [21, 22]. Since we are interested in ferromagnetic BECs, we assume $c_1 < 0$ in this paper. Spin-1 ^{87}Rb atoms are known to be ferromagnetic. The quadratic Zeeman effect introduces an easy plane ($q > 0$) or an easy axis ($q < 0$) of the spontaneous magnetization. As seen from Eq. (3), the quadratic Zeeman effect enhances the population in the $m = 0$ state for $q > 0$ and those in the $m = \pm 1$ state for $q < 0$. Suppose that the quadratic Zeeman effect is much weaker than the ferromagnetic interaction. Then, the condensate is fully-magnetized. Because the order parameter for a fully-magnetized state in the direction $(\cos \alpha \sin \beta, \sin \alpha \sin \beta, \cos \beta)$ is given by [10, 12]

$$\Psi \equiv \begin{pmatrix} \Psi_1 \\ \Psi_0 \\ \Psi_{-1} \end{pmatrix} = \sqrt{n_{\text{tot}}} e^{i\phi} \begin{pmatrix} e^{-i\alpha} \cos^2 \frac{\beta}{2} \\ \sqrt{2} \sin \frac{\beta}{2} \cos \frac{\beta}{2} \\ e^{i\alpha} \sin^2 \frac{\beta}{2} \end{pmatrix}, \quad (8)$$

the population in the $m = 0$ component becomes maximum at $\beta = \pi/2$, whereas those in the $m = 1$ and -1 component becomes maximum at $\beta = 0$ and π , respectively. Hence, the magnetization arises in the x - y plane for $q > 0$ and in the $+z$ or $-z$ direction for $q < 0$. The former case corresponds to the XY model and the latter the Ising model.

Now, we move to dynamics. The dynamics of a spinor BEC is well described with the time-dependent multi-component GP equation [10]:

$$i\hbar \frac{\partial}{\partial t} \Psi_m(\mathbf{r}, t) = \frac{\delta(\mathcal{E} - N\mu)}{\delta \Psi_m^*(\mathbf{r}, t)}, \quad (9)$$

where μ is the chemical potential. We phenomenologically introduce an energy dissipation by replacing $i\partial/\partial t$ in Eq. (9) with $(i - \Gamma)\partial/\partial t$ [23]. Under this replacement, the chemical potential becomes time-dependent so as to conserve the total number of atoms. Then, using Eqs. (1)–(3) and (5), we obtain the dissipative GP equa-

tion as

$$\begin{aligned}
& (i - \Gamma)\hbar\frac{\partial}{\partial t}\Psi_m(\mathbf{r}, t) \\
&= \left[-\frac{\hbar^2}{2M}\nabla^2 + U_{\text{trap}}(\mathbf{r}) - \mu(t) \right. \\
&\quad \left. + qm^2 + c_0n_{\text{tot}}(\mathbf{r}, t) \right] \Psi_m(\mathbf{r}, t) \\
&\quad + c_1 \sum_{n=-1}^1 \sum_{\nu=x,y,z} f_\nu(\mathbf{r}, t)(F_\nu)_{mn} \Psi_n(\mathbf{r}, t). \quad (10)
\end{aligned}$$

We consider the low energy limit that the kinetic energy arising from the spatial variation of the order parameter Ψ_m is much smaller than both the spin-dependent (c_1) and spin-independent (c_0) interactions. We also assume that the quadratic Zeeman energy is much smaller than the interatomic interactions. Under the above assumptions, the BEC can be treated as a fully magnetized gas, namely, the amplitude of the spin density is given by $|\mathbf{f}| = n_{\text{tot}}$ and only its direction varies in space. In such a situation, the physical quantities that describe the dynamics of the ferromagnetic BEC are the normalized spin vector

$$\hat{\mathbf{f}} \equiv \frac{\mathbf{f}}{n_{\text{tot}}}, \quad (11)$$

and the superfluid velocity \mathbf{v}_{mass} , which is defined as the sum of currents in all spin components:

$$n_{\text{tot}}\mathbf{v}_{\text{mass}} \equiv \frac{\hbar}{2Mi} \sum_{m=-1}^1 [\Psi_m^*(\nabla\Psi_m) - (\nabla\Psi_m^*)\Psi_m]. \quad (12)$$

The equations of motion for these physical quantities are derived straightforwardly from the GP equation (10). The detailed derivation is given in Refs. [12, 16], and the resulting equations of motion are written as

$$\begin{aligned}
\frac{\partial \hat{\mathbf{f}}}{\partial t} &= \frac{1}{1 + \Gamma^2} \left[\frac{1}{\hbar} \hat{\mathbf{f}} \times \mathbf{B}_{\text{eff}} - (\mathbf{v}_{\text{mass}} \cdot \nabla) \hat{\mathbf{f}} \right] \\
&\quad - \frac{\Gamma}{1 + \Gamma^2} \hat{\mathbf{f}} \times \left[\frac{1}{\hbar} \hat{\mathbf{f}} \times \mathbf{B}_{\text{eff}} - (\mathbf{v}_{\text{mass}} \cdot \nabla) \hat{\mathbf{f}} \right], \quad (13a)
\end{aligned}$$

$$\mathbf{B}_{\text{eff}} = \frac{\hbar^2}{2M}\nabla^2 \hat{\mathbf{f}} + \frac{\hbar^2}{2M}(\mathbf{a} \cdot \nabla) \hat{\mathbf{f}} - q\hat{f}_z \hat{\mathbf{z}}, \quad (13b)$$

$$\begin{aligned}
M\frac{\partial}{\partial t}\mathbf{v}_{\text{mass}} &= \frac{\hbar}{2n_{\text{tot}}\Gamma} \nabla [\nabla \cdot (n_{\text{tot}}\mathbf{v}_{\text{mass}})] \\
&\quad + \hbar(\nabla \hat{\mathbf{f}}) \cdot \left(\hat{\mathbf{f}} \times \frac{\partial \hat{\mathbf{f}}}{\partial t} \right), \quad (13c)
\end{aligned}$$

where $\mathbf{a} = (\nabla n_{\text{tot}})/n_{\text{tot}}$. Here, the first term in the right-hand side of Eq. (13c) does not diverge at $\Gamma = 0$

since $\nabla \cdot (n_{\text{tot}}\mathbf{v}_{\text{mass}}) \propto \Gamma$: Eq. (13c) is also written as [16]

$$M\frac{\partial}{\partial t}\mathbf{v}_{\text{mass}} = -\nabla [\mu_{\text{local}} - \mu(t)] + \hbar(\nabla \hat{\mathbf{f}}) \cdot \left(\hat{\mathbf{f}} \times \frac{\partial \hat{\mathbf{f}}}{\partial t} \right), \quad (14)$$

where

$$\mu_{\text{local}} - \mu(t) = \frac{M}{2}\mathbf{v}_{\text{mass}}^2 + \frac{\hbar^2}{4M}(\nabla \hat{\mathbf{f}})^2 - \frac{\hbar^2}{2M} \frac{\nabla^2 \sqrt{n_{\text{tot}}}}{\sqrt{n_{\text{tot}}}}. \quad (15)$$

In the following sections, we investigate the spin dynamics in a ferromagnetic BEC using both Eqs. (10) and (13). We discuss especially the Ising-like case ($q < 0$). In this case, the assumption for the spin-dependent interaction to derive the hydrodynamic equation is weakened: we only require that the kinetic energy arising from spin textures is negligible compared with the spin-dependent interaction *or* the quadratic Zeeman energy, since both terms favor the ferromagnetic state. Note, however, that when the quadratic Zeeman energy dominates the spin-dependent interaction ($|c_1 n_{\text{tot}}| \lesssim |q|$) the magnetization vanishes inside domain walls. We consider a quasi-2D system perpendicular to the z direction (the direction of the applied magnetic field), i.e., the Thomas-Fermi radius in the z direction is smaller than the spin healing length ($\xi_{\text{sp}} \equiv \hbar/\sqrt{2M|c_1|n_{\text{tot}}}$), so that magnetic structure in the z direction is uniform. For simplicity, we neglect the confining potential in the x - y plane and set $\mathbf{a} = \mathbf{0}$.

III. DOMAIN GROWTH

The domain growth laws in the Ising model and binary fluids have been well investigated experimentally, theoretically, and numerically. Here, we briefly review the growth laws in those models especially in two dimension, and discuss what growth laws are expected to be in 2D ferromagnetic BECs.

The free energy for a continuum description of the 2D Ising model is written as

$$F[\phi] = \int d^2x \left[\frac{1}{2} |\nabla \phi|^2 + V(\phi) \right], \quad (16)$$

where ϕ is an order parameter and $V(\phi)$ is a double-well potential, e.g., $V(\phi) = (1 - \phi^2)^2$. When the order parameter is not conserved, the time evolution of ϕ is given by the time-dependent Ginzburg-Landau (TDGL) equation,

$$\frac{\partial \phi}{\partial t} = -\frac{\delta F}{\delta \phi} = \nabla^2 \phi - \frac{dV}{d\phi}. \quad (17)$$

This equation implies that the rate of change in the order parameter is proportional to the gradient of the free energy. In this case, domain growth is driven by the surface tension of domain walls. Domain wall velocity dl/dt ,

where l is the characteristic length of domain, is approximately proportional to the curvature $K \sim 1/l$ of the domain wall. Thus, domains grow as $l(t) \sim t^{1/2}$ at late times, when the interaction between domain walls are negligible. This domain growth law for 2D non-conserved scalar fields has been confirmed in more sophisticated ways [1, 3].

When the order parameter is conserved, domain growth is mainly caused by the diffusive transport of ϕ . In this case, a continuity equation, $\partial\phi/\partial t = -\nabla \cdot \mathbf{j}$, where $\mathbf{j} = -\lambda\nabla(\delta F/\delta\phi)$, leads to the Cahn-Hilliard equation,

$$\begin{aligned} \frac{\partial\phi}{\partial t} &= \lambda\nabla^2 \frac{\delta F}{\delta\phi} \\ &= -\lambda\nabla^2 \left[\nabla^2\phi - \frac{dV}{d\phi} \right]. \end{aligned} \quad (18)$$

Here, λ is the transport coefficient. The Cahn-Hilliard equation is often used to describe the dynamics of phase separation in conserved systems. The domain growth law for 2D conserved field is $l \sim t^{1/3}$, which has been derived in several ways [1, 2, 4].

In binary fluids, the transport of ϕ is caused by hydrodynamic flow as well as diffusion. Thus, Eq. (18) is modified as

$$\frac{\partial\phi}{\partial t} + \mathbf{v} \cdot \nabla\phi = \lambda\nabla^2\mu, \quad (19)$$

where \mathbf{v} is the local fluid velocity, and $\mu \equiv \delta F/\delta\phi$ is the chemical potential. The velocity obeys the Navier-Stokes equation. In the incompressible limit, it is written by

$$\rho \left(\frac{\partial\mathbf{v}}{\partial t} + (\mathbf{v} \cdot \nabla)\mathbf{v} \right) = \eta\nabla^2\mathbf{v} - \nabla p - \phi\nabla\mu, \quad (20)$$

where p is the pressure, η is the viscosity, and the density ρ is constant. The left hand side of Eq. (20), which is inertial terms, vanishes in the overdamped limit. When the inertial terms are negligible compared with the viscous force, we shall say the system is in the viscous hydrodynamic regime. The domain growth law is $l(t) \sim t$ in the viscous hydrodynamic regime [5], which has been confirmed by experiments as well as numerical simulations [1]. In contrast, if the inertial terms are important, the system is in the inertial hydrodynamic regime. The domain growth law for the inertial hydrodynamic regime is $l(t) \sim t^{2/3}$ [6]. However, in classical fluids, the viscous term is usually non-negligible, and the scaling law $l \sim t^{2/3}$ is hard to be observed in experiments.

In a ferromagnetic BEC, if the total magnetization in the z -direction is initially zero, the z -component of magnetization is a conserved order parameter. Thus, if $\mathbf{v}_{\text{mass}} = 0$, the expected domain growth law is $l(t) \sim t^{1/3}$, which is confirmed by the hydrodynamic simulations for no- \mathbf{v}_{mass} cases in Sec. IV. The superfluid flow in a ferromagnetic BEC corresponds to the hydrodynamic flow in binary liquids. Since the viscosity vanishes in a BEC, the domain growth law in a ferromagnetic BEC is expected to

be the same as that of the inertial hydrodynamic regime: $l(t) \sim t^{2/3}$. This expectation is confirmed by GP and hydrodynamic simulations is Sec. IV.

IV. NUMERICAL SIMULATIONS

We define the characteristic length of magnetic domains by means of scattering structure factor,

$$S_z(\mathbf{k}) = \langle \tilde{f}_z(\mathbf{k}) \tilde{f}_z(-\mathbf{k}) \rangle, \quad (21)$$

where $\langle \dots \rangle$ represents a spacial average and $\tilde{f}_z(\mathbf{k})$ is the Fourier transform of $f_z(\mathbf{r})/n_{\text{tot}}$. The characteristic length of magnetic domains, i.e., domain size, l is defined by $l \equiv \pi/k^*$, where k^* is the first moment of $S_z(k)$, which is the azimuth average of $S_z(\mathbf{k})$:

$$k^* \equiv \frac{\int_0^\infty dk k S_z(k)}{\int_0^\infty dk S_z(k)}. \quad (22)$$

We perform numerical simulations mainly by the GP equation. Simulations by the hydrodynamic equations are also performed to investigate the effects of \mathbf{v}_{mass} . The mass of an atom is given by a typical value for a spin-1 ^{87}Rb atom: $M = 1.44 \times 10^{-25}$ Kg. In GP simulations, the system is in quasi-two dimension: the wave function in the normal direction to the 2D plane is approximated by a Gaussian with width d . The total number density is taken as $n_{\text{tot}} = \sqrt{2\pi d^2} n_{3\text{D}}$ with $n_{3\text{D}} = 2.3 \times 10^{14}$ cm $^{-3}$ and $d = 1$ μm .

Initial states are given as $f_x/n_{\text{tot}} = 1$, $f_y = f_z = 0$ with additional small noises, and periodic boundary conditions are imposed on 512 $\mu\text{m} \times 512$ μm systems. The quadratic Zeeman energy is set to be a negative value so that domains of longitudinal magnetization ($f_z/n_{\text{tot}} = \pm 1$) arise.

In the GP simulations, we use the interaction parameters $c_0 n_{3\text{D}}/h = 1.3$ kHz and $c_1 n_{3\text{D}} = -5.9$ Hz. Figure 1 shows the time evolution of the spatial average of transverse magnetization $|F_+| = \sqrt{f_x^2 + f_y^2}/n_{\text{tot}}$, that of magnetization rate $|\mathbf{f}|/n_{\text{tot}}$, and that of longitudinal magnetization f_z/n_{tot} obtained by the GP simulations. In early times, the magnetization arises mainly in the x - y plane and its amplitude oscillates due to the quadratic Zeeman effect. At around $t = 0.2$ – 0.6 s, the longitudinal magnetization increases rapidly and the amplitude oscillations of the longitudinal magnetization appear just after the rapid growth. The oscillations induce the oscillations of domain size in Fig. 2. Well-defined domains are available at $t \gtrsim 1$ s. The time dependence of domain size $l(t)$ is shown in Fig. 2. When domains are well developed at $t \gtrsim 1$ s, domains grow as $l(t) \sim t^{2/3}$, which coincide with the domain growth law for 2D binary fluid in the inertial hydrodynamic regime.

The quadratic Zeeman energy determines the domain-wall structure: the domain walls are transversely magnetized for $|q| \lesssim |c_1 n_{3\text{D}}|$, whereas the magnetization vanishes inside the domain wall for $|q| \gtrsim |c_1 n_{3\text{D}}|$. The result

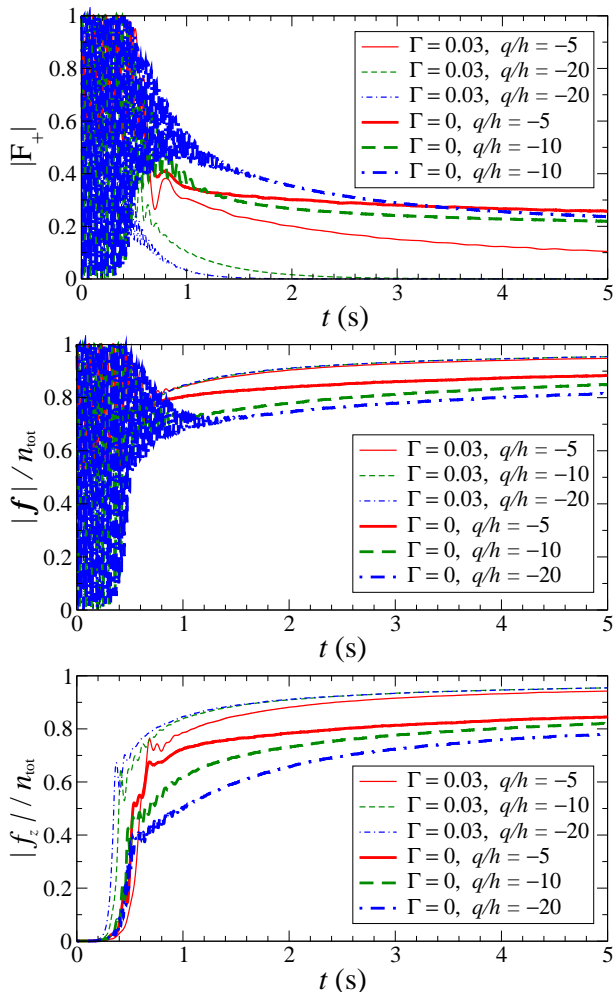


FIG. 1. (Color online) Time dependences of the spatial average of transverse magnetization $|F_+|$, that of magnetization rate $|f|/n_{\text{tot}}$, and that of longitudinal magnetization $|f_z|/n_{\text{tot}}$ in the GP simulations. Each curve is the ensemble average of 5 simulations.

in Fig. 2 that the growth law does not depend on the value of q means that the domain-wall structure does not affect the growth law.

In Figs. 1 and 2, we perform calculations in both the dissipative ($\Gamma = 0.03$) and nondissipative ($\Gamma = 0$) cases and obtain the same growth law $l(t) \sim t^{2/3}$. The apparent difference between those cases is the average domain size: the domain size of the dissipative case is larger than that of the nondissipative case. When domains grow, the energy associated with domain walls decreases effectively in the dissipative case. In other words, energy dissipation promotes domain growth. In the nondissipative case, the decrease of the domain-wall energy cannot be caused by dissipation, although domains can still grow converting the domain-wall energy to other energies. Actually, as shown in Fig. 1, the transverse magnetization remains larger and the magnetization rate remains lower for the nondissipative cases than the dissipative cases, indicating

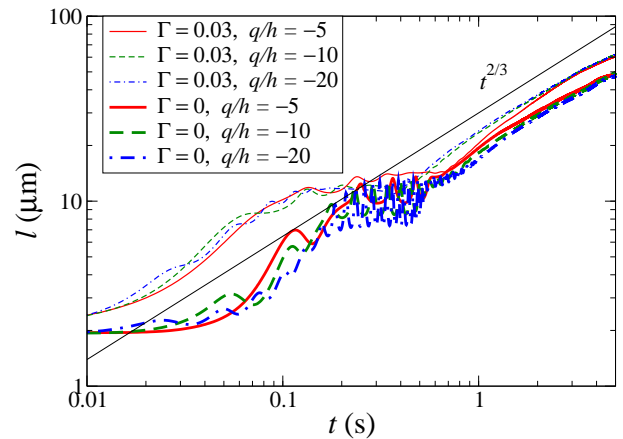


FIG. 2. (Color online) Time dependence of domain size $l(t)$ in the GP simulations. Each curve is the ensemble average of 5 simulations.

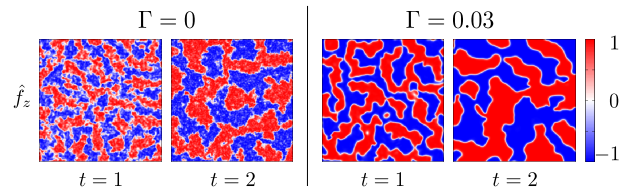


FIG. 3. (Color online) Snapshots of longitudinal magnetization f_z/n_{tot} obtained by the GP simulations. The size of each snapshot is $300 \mu\text{m}$ on each side.

that the decrease in the domain-wall energy is compensated with the increase in the quadratic Zeeman energy and the ferromagnetic interaction energy.

Snapshots of longitudinal magnetization f_z/n_{tot} in both dissipative ($\Gamma = 0.03$) and nondissipative ($\Gamma = 0$) cases are demonstrated in Fig. 3. The snapshot for $\Gamma = 0$ at $t = 2$, where small white fractions still remains inside domains, reflects the fact that transverse magnetization does not vanish even in late times for $\Gamma = 0$.

In order to investigate the effects of superfluid flow, we have performed simulations by means of the hydrodynamic equations in the presence and in the absence of \mathbf{v}_{mass} . The time dependences of domain size $l(t)$ in fully-hydrodynamic and no- \mathbf{v}_{mass} simulations are shown in Figs. 4(a) and 4(b), respectively. In the fully-hydrodynamic cases, as seen in Fig. 4(a), domains grow as $l(t) \sim t^{2/3}$, which is the same growth law as in the GP simulations. Figure 4(b) indicates that the growth law in no- \mathbf{v}_{mass} cases coincides with that of 2D conserved scalar fields: $l(t) \sim t^{1/3}$. The dependences on q and Γ are not noticeable.

The time dependence of transverse magnetization in the hydrodynamic simulations, which is shown in Fig. 5, shows similar tendency to that in the GP simulations: the transverse magnetization remains larger in the nondissipative cases than the dissipative cases. The difference between dissipative and nondissipative cases is larger

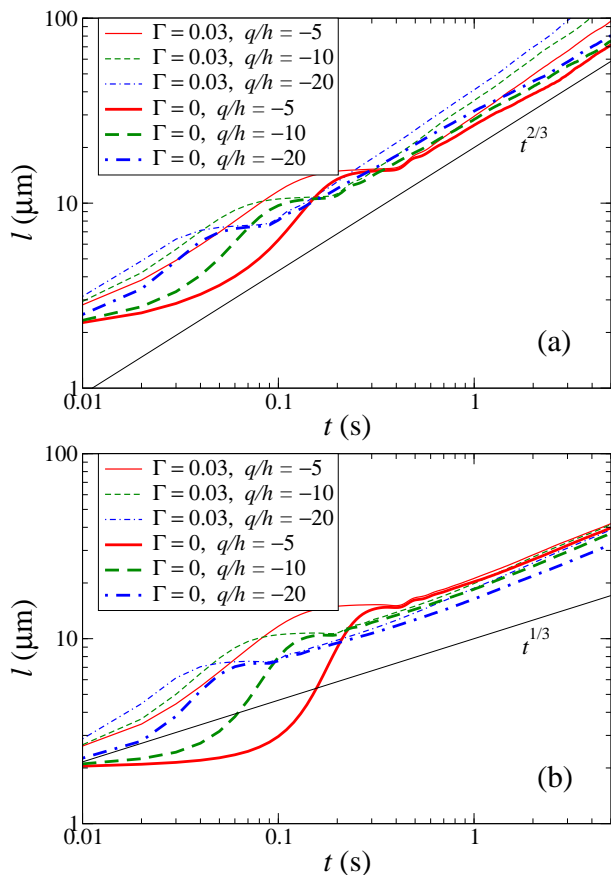


FIG. 4. (Color online) Time dependence of domain size $l(t)$ obtained by the hydrodynamic simulations (a) with \mathbf{v}_{mass} and (b) without \mathbf{v}_{mass} . Each curve is the ensemble average of 5 simulations.

in Fig. 5(a) than Fig. 5(b). Since the magnitude of transverse magnetization is related with the loss of the domain-wall energy, this is consistent with the results in Fig. 4, i.e., the difference in domain size between dissipative and nondissipative cases is larger in the fully-hydrodynamic simulations than the no- \mathbf{v}_{mass} simulations.

Figure 6 shows the snapshots of \hat{f}_z in (a) fully-hydrodynamic and (b) no- \mathbf{v}_{mass} simulations. Domain size is apparently larger in (a) than (b), which is in good agreement with the results in Fig. 4.

Finally, we discuss the effect of a confining potential, which is unavoidable in experiments, on the growth law. The effect of the confining potential is to cause a non-uniform density profile n_{tot} . Since the spin-independent interaction is much stronger than the spin-dependent interaction, this density distribution is not affected by spin structures, and thus, does not evolve in time. Such a time-independent term does not contribute to the scaling behavior of domain growth. Hence, the growth law is expected not to change even in the presence of a confining potential.

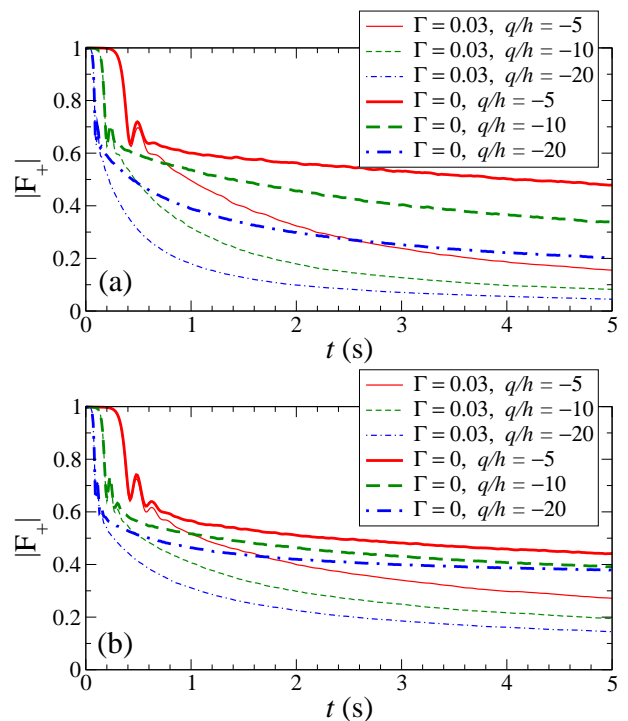


FIG. 5. (Color online) Time dependences of the spatial average of transverse magnetization $|F_+|$ in (a) fully-hydrodynamic and (b) no- \mathbf{v}_{mass} simulations. Each curve is the ensemble average of 5 simulations.

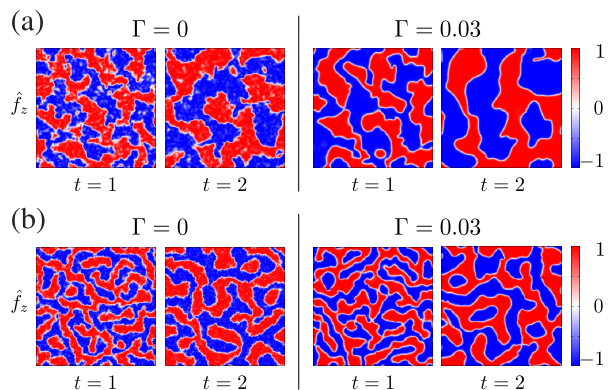


FIG. 6. (Color online) Snapshots of longitudinal magnetization \hat{f}_z in (a) fully-hydrodynamic and (b) no- \mathbf{v}_{mass} simulations. The size of each snapshot is $300 \mu\text{m}$ on each side.

V. CONCLUSIONS

We have performed the GP and hydrodynamic simulations to investigate the effects of the superfluid flow on the magnetic domain growth in ferromagnetic BECs with negative quadratic Zeeman energies. Domain patterns formed by the longitudinal magnetization grow as time evolves. The characteristic domain size grows, as expected, as $l(t) \sim t^{2/3}$ in the GP and the fully-hydrodynamic simulations and $l(t) \sim t^{1/3}$ in the hydro-

dynamics simulations without the superfluid flow. The former and the latter correspond to the growth laws for diffusive and inertial hydrodynamic dynamics in conserved scalar fields, respectively. The domain growth laws are almost independent of the quadratic Zeeman energy and dissipation, although domain size increases earlier in the dissipative case than the nondissipative case especially in the GP and the fully-hydrodynamic simulations.

In conclusion, the superfluid flow promotes the magnetic domain growth in ferromagnetic BECs. The growth laws for negative quadratic Zeeman energy are the same

as those of conserved scalar fields and are independent of the quadratic Zeeman energy and dissipation.

ACKNOWLEDGMENTS

This work was supported by KAKENHI (22340114, 22740265, 22103005) from MEXT of Japan, and by Funding Program for World-Leading Innovation R & D on Science and Technology (FIRST). YK acknowledges the financial support from Inoue Foundation for Science.

-
- [1] A. J. Bray, *Adv. Phys.* **43**, 357 (1994).
 - [2] I. M. Lifshitz and V. V. Slyozov, *J. Phys. Chem. Solids* **19**, 35 (1961).
 - [3] T. Ohta, D. Jasnow, and K. Kawasaki, *Phys. Rev. Lett.* **49**, 1223 (1982).
 - [4] D. A. Huse, *Phys. Rev. B* **34**, 7845 (1986).
 - [5] E. D. Siggia, *Phys. Rev. A* **20**, 595 (1979).
 - [6] H. Furukawa, *Phys. Rev. A* **31**, 1103 (1985).
 - [7] L. E. Sadler, J. M. Higbie, S. R. Leslie, M. Vengalattore, and D. M. Stamper-Kurn, *Nature* **443**, 312 (2006).
 - [8] M. Vengalattore, S. R. Leslie, J. Guzman, and D. M. Stamper-Kurn, *Phys. Rev. Lett.* **100**, 170403 (2008).
 - [9] M. Vengalattore, J. Guzman, S. R. Leslie, F. Serwane, and D. M. Stamper-Kurn, *Phys. Rev. A* **81**, 053612 (2010).
 - [10] K. Kawaguchi and M. Ueda, *Phys. Rep.* **520**, 253 (2012).
 - [11] A. Lamacraft, *Phys. Rev. A* **77**, 063622 (2008).
 - [12] K. Kudo and Y. Kawaguchi, *Phys. Rev. A* **82**, 053614 (2010).
 - [13] E. Yukawa and M. Ueda, *Phys. Rev. A* **86**, 063614 (2012).
 - [14] R. Barnett, D. Podolsky, and G. Refael, *Phys. Rev. B* **80**, 024420 (2009).
 - [15] R. W. Cherng and E. Demler, *Phys. Rev. A* **83**, 053613 (2011); R. W. Cherng and E. Demler, *Phys. Rev. A* **83**, 053614 (2011).
 - [16] K. Kudo and Y. Kawaguchi, *Phys. Rev. A* **84**, 043607 (2011).
 - [17] J. C. Slonczewski, *J. Magn. Magn. Mater.* **159**, L1 (1996); L. Berger, *Phys. Rev. B* **54**, 9353 (1996).
 - [18] Ya. B. Bazaliy, B. A. Jones, and S.-C. Zhang, *Phys. Rev. B* **57**, R3213 (1998); Z. Li and S. Zhang, *Phys. Rev. Lett.* **92**, 207203 (2004).
 - [19] J. Guzman, G.-B. Jo, A. N. Wenz, K. W. Murch, C. K. Thomas, and D. M. Stamper-Kurn, *Phys. Rev. A* **84**, 063625 (2011).
 - [20] F. Gerbier, A. Widera, S. Folling, O. Mandel, I. Bloch, *Phys. Rev. A* **73**, 041602(R) (2006).
 - [21] T.-L. Ho, *Phys. Rev. Lett.* **81**, 742 (1998).
 - [22] T. Ohmi and K. Machida, *J. Phys. Soc. Jpn.* **67**, 1822 (1998).
 - [23] M. Tsubota, K. Kasamatsu, and M. Ueda, *Phys. Rev. A* **65**, 023603 (2002); K. Kasamatsu, M. Tsubota, and M. Ueda, *Phys. Rev. A* **67**, 033610 (2003).